

See discussions, stats, and author profiles for this publication at: <https://www.researchgate.net/publication/263952340>

# Understanding Trends in CO<sub>2</sub> Adsorption in Metal–Organic Frameworks with Open–Metal Sites

ARTICLE *in* JOURNAL OF PHYSICAL CHEMISTRY LETTERS · FEBRUARY 2014

Impact Factor: 7.46 · DOI: 10.1021/jz500202x

---

CITATIONS

19

---

READS

55

5 AUTHORS, INCLUDING:



**Roberta Poloni**

Grenoble Institute of Technology

34 PUBLICATIONS 432 CITATIONS

SEE PROFILE



**Kyuho Lee**

University of California, Berkeley

46 PUBLICATIONS 1,623 CITATIONS

SEE PROFILE



**Berend - Smit**

University of California, Berkeley

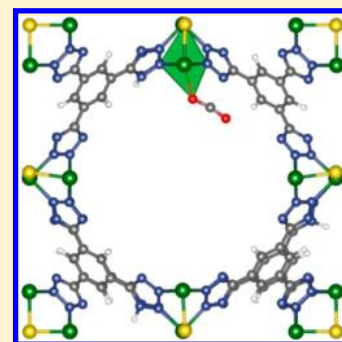
346 PUBLICATIONS 18,734 CITATIONS

SEE PROFILE

Understanding Trends in CO<sub>2</sub> Adsorption in Metal–Organic Frameworks with Open-Metal SitesRoberta Poloni,<sup>\*,†,‡,§</sup> Kyuho Lee,<sup>‡,§</sup> Robert F. Berger,<sup>§,#</sup> Berend Smit,<sup>‡</sup> and Jeffrey B. Neaton<sup>\*,§,||,⊥</sup><sup>†</sup>Laboratoire Science et Ingénierie des Matériaux et Procédés (SIMaP), Grenoble-INP, UMR CNRS-5266, 1130 rue de la Piscine, 38402 Saint Martin d'Hères, France<sup>‡</sup>Department of Chemical and Biomolecular Engineering, University of California, 201 Gilman Hall, Berkeley, California 94720, United States<sup>§</sup>Molecular Foundry, Lawrence Berkeley National Laboratory, One Cyclotron Road, Berkeley, California 94720, United States<sup>||</sup>Department of Physics, University of California, Berkeley, 366 LeConte Hall MC 7300, Berkeley, California 94720, United States<sup>⊥</sup>Kavli Energy NanoSciences Institute at Berkeley, Berkeley, California 94720, United States

## S Supporting Information

**ABSTRACT:** Using van der Waals-corrected density functional theory and a local chemical bond analysis, we study and explain trends in the binding between CO<sub>2</sub> and open-metal coordination sites within a series of two metal–organic frameworks (MOFs), BTT, and MOF-74 for Ca, Mg, and nine divalent transition-metal cations. We find that Ti and V result in the largest CO<sub>2</sub> binding energies and show that for these cations the CO<sub>2</sub> binding energies for both structure types are twice the value expected based on pure electrostatics. We associate this behavior with the specific electronic configuration of the divalent cations and symmetry of the metal coordination site upon CO<sub>2</sub> binding, which result in empty antibonding orbitals between CO<sub>2</sub> and the metal cation. We demonstrate that a chemical bond analysis and electrostatic considerations can be used to predict trends of CO<sub>2</sub> binding affinities to MOFs with transition-metal cations.



**SECTION:** Molecular Structure, Quantum Chemistry, and General Theory

Climate change due to anthropogenic emissions of CO<sub>2</sub> is now well accepted, and several initiatives have been proposed to reduce such emissions.<sup>1</sup> These include, among others, the increase in the use of renewable energy and the improvement of the efficiency and conservation of fossil fuel resources, including a significant contribution from CO<sub>2</sub> capture and storage (CCS).<sup>2</sup> Among the different candidate approaches that enable more efficient separations of CO<sub>2</sub> from other gases, physisorption by metal–organic frameworks (MOFs) is one of the most promising.<sup>3–6</sup> MOFs are 3-D nanoporous extended solids composed of metal centers connected by organic molecules, called bridging ligands. Their high surface area, high CO<sub>2</sub> selectivity, and chemical tunability<sup>6,7</sup> can allow for the design of optimum materials for carbon capture. In particular, MOFs exhibiting coordinatively unsaturated metal centers have been observed to provide promising selectivity of CO<sub>2</sub> over N<sub>2</sub> and a high CO<sub>2</sub> capacity at very low pressures,<sup>8</sup> which is relevant for efficient gas separations from a postcombustion process. Improving CO<sub>2</sub> capacity of these materials would be desirable, and a way to achieve this is by increasing the interaction energy with the metal center. For this reason, several studies have quantified changes in the CO<sub>2</sub> heat of adsorption when replacing the metal atom for a given MOF topology.<sup>8–14</sup> Interestingly, a large binding strength has been computed for early transition metals, for example, Ti and V, which are found to bind differently than

expected from their size and nominal charge state.<sup>13,14</sup> However, chemical intuition is still missing for why these metal cations lead to strong CO<sub>2</sub> binding or selectivity, and such intuition is needed for guiding further experimental efforts.

Here, we calculate MOF–CO<sub>2</sub> binding energies using density functional theory (DFT) with van der Waals dispersion corrections,<sup>15</sup> explaining computed trends in open-metal sites using electrostatic arguments and a local chemical bond analysis. We focus on a class of recently synthesized sodalite-type frameworks called M-BTT (H<sub>3</sub>[(M<sub>4</sub>Cl)<sub>3</sub>(BTT)<sub>8</sub>], M = M<sup>2+</sup> metal, BTT = 1,3,5-benzenetristetrazolate)<sup>16–19</sup> possessing coordinatively unsaturated metal centers, which, in prior work,<sup>20</sup> have been shown to exhibit promising CO<sub>2</sub> binding energies that are sensitive to the choice of the metal (Mg, Ca, Sr, and Cu) and ligand (tetrazole, triazole and oxazole).<sup>20</sup> Examining CO<sub>2</sub> binding across a range of first-row transition-metal cations within BTT-type frameworks, we predict binding energies ranging from 32.2 kJ/mol for Cu to 80.2 kJ/mol for V. We show that for Ti and V, the trend in CO<sub>2</sub> binding energy deviates significantly from expectations based on the formal charge of the cation and the metal–oxygen distance (or ionic

Received: January 29, 2014

Accepted: February 13, 2014

Table 1. CO<sub>2</sub> Adsorption (Binding) Energies and Geometries Computed with DFT+D2<sup>a</sup>

metal	$E_{\text{ads}}$ (kJ/mol)	O–C–O (deg)	O–M (Å)	C–N (Å)	$\mu$ ( $\mu_{\text{B}}$ )	$Q$	$a$ (Å)
Mg	67.2	172.1	2.207	2.605		1.10	19.010
Ca	60.6	173.6	2.475	2.758		1.20	19.646
Ti	73.2	171.3	2.237	2.660	1.48	0.77	18.973 1
V	80.2	170.0	2.188	2.648	2.82	0.69	18.832
Cr	36.6	175.5	2.747	2.781	3.90	0.59	18.769
Mn	50.8	174.2	2.401	2.732	4.82	0.90	19.073
Fe	47.3	173.8	2.405	2.720	3.66	0.78	18.909
Co	39.0	174.8	2.521	2.732	0.98	0.54	18.350
Ni	38.9	174.7	2.567	2.756	1.40	0.60	18.502
Cu	32.2	176.0	2.752	2.809	0.52	0.55	18.743
Zn	43.2	174.5	2.441	2.726		0.71	18.909

<sup>a</sup>CO<sub>2</sub> adsorption energies computed using a van der Waals-corrected functional (DFT+D2) for BTT MOFs and corresponding bond distances and the bond angle of CO<sub>2</sub>. The metal magnetic moment, metal Mulliken charges,  $Q$ , in units of electron, and the lattice parameter for the bare frameworks, also computed using DFT+D2, are reported here. An antiferromagnetic ordering and high spin configuration is predicted for all systems considered, except Co-BTT. Zero point and thermal contributions are neglected.

radius). The electronic configurations of these metals ( $d^2$  and  $d^3$ ) result in empty antibonding  $\sigma^*$  states between the CO<sub>2</sub> and the metal cation, which are populated for cations with a greater number of  $d$  electrons (Cr and later); the empty  $\sigma^*$  antibonding states can thus be connected to the predicted enhanced binding energy. More generally, our study demonstrates that a chemical bond analysis and electrostatic considerations can be used to predict trends of CO<sub>2</sub> binding affinities to MOFs with transition-metal cations and suggests that MOFs synthesized with early transition-metal open sites will lead to significantly enhanced molecular adsorption.

Our DFT calculations are performed within the generalized gradient approximation,<sup>21</sup> van der Waals dispersion corrections are treated with the Grimme method (DFT+D2).<sup>15</sup> We use the SIESTA package,<sup>22</sup> a localized atomic orbital basis, and norm-conserving pseudopotentials for all calculations. (See the SI for details.) Adsorption energies neglect zero-point energy and thermal contributions (binding energies). In recent calculations,<sup>23</sup> thermal contributions at room temperature, together with zero-point energies, reduce the CO<sub>2</sub> binding energy by  $\sim 5$  kJ/mol. The binding energies reported here have been obtained without a Hubbard  $U$  correction; results obtained using DFT+ $U$  are reported in the SI. Although we find that they can vary in magnitude by  $\sim 8$  kJ/mol with choice of  $U$  (see SI), such corrections do not change the trends described here.

The CO<sub>2</sub> binding geometry in M-BTT MOFs is similar for all metal cations and has already been described in detail in previous work.<sup>20</sup> A three-site interaction between the CO<sub>2</sub> and the MOF, where the CO<sub>2</sub> oxygen atoms interact with both the hydrogen and metal atoms of the framework, respectively, leads to the CO<sub>2</sub> carbon atom being concomitantly attracted to the negatively charged nitrogen of the tetrazole ligand, as illustrated in our recent work.<sup>20</sup> In Table 1, we report computed binding energies, optimized binding geometries, the lattice parameter of the bare MOF, the metal Mulliken charge,  $Q$ , and the magnetic moment,  $\mu$ , of the metal cation in the bare framework. The lattice parameter correlates well with the ionic radii of the metal ions, in agreement with recent diffraction studies for Mn-BTT,<sup>16</sup> Fe-BTT,<sup>19</sup> and Cu-BTT,<sup>24</sup> where cell parameters of 19.116,<sup>16</sup> 18.824,<sup>19</sup> and 18.595 Å,<sup>24</sup> respectively, are reported for the solvated MOFs. Our calculations led to a binding energy of 21.7 kJ/mol<sup>20</sup> for a similar MOF, Cu-BTTri (BTTri = 1,3,5-tri(1H-1,2,3-triazol-4-yl)benzene), in good agreement with the value of 21 kJ/mol computed from the temperature depend-

ence of the adsorption isotherm.<sup>18</sup> As mentioned, zero-point and thermal corrections will tend to reduce our adsorption energy by no more than a few kilojoules per mole.

Binding energies correlate with CO<sub>2</sub>–metal bond distances and angles: larger binding corresponds to a shorter bond distance and a smaller CO<sub>2</sub> bond angle. The bond distance between the CO<sub>2</sub> carbon and the tetrazole nitrogen decreases with increasing binding energy, although the computed charge on the nitrogen is fairly constant. This is due to the larger induced polarization of CO<sub>2</sub>, which results in a stronger bond between the nitrogen and the more positively charged carbon of CO<sub>2</sub>. The CO<sub>2</sub> binding energy for V and Ti is significantly larger compared with the other transition-metal atoms, as also observed in other MOFs in recent studies.<sup>13,14</sup>

Figure 1 summarizes computed trends in  $Q/r$ , a measure of the strength of the electrostatic contribution to CO<sub>2</sub> binding, as

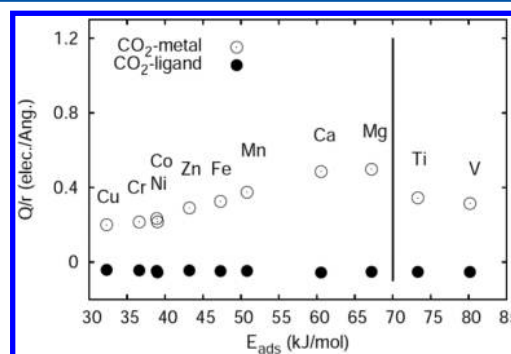
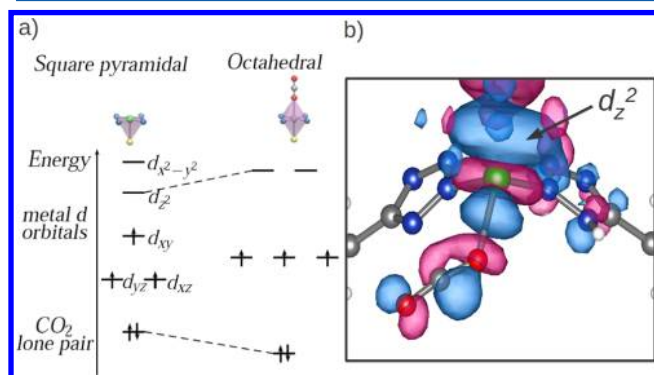


Figure 1. CO<sub>2</sub> adsorption energy plotted over  $Q/r$  computed for the metal–CO<sub>2</sub> oxygen distance and the tetrazole nitrogen–CO<sub>2</sub> carbon distance. The vertical line is to guide the eye.

a function of MOF–CO<sub>2</sub> binding energy for the different metal cations. Here  $Q$  is either the Mulliken charge of metal atom or ligand nitrogen closest to CO<sub>2</sub> (see Figure 1), computed from a bare MOF. The distance,  $r$ , is either the CO<sub>2</sub> oxygen–metal or CO<sub>2</sub> carbon–ligand nitrogen separation, respectively. From Figure 1, the ligand contribution can be seen to be roughly independent of metal cation; the CO<sub>2</sub>–metal  $Q/r$  plot, however, shows a strong, positive correlation between binding energy and  $Q/r$ , with the exception of Ti and V, which exhibit a much stronger binding energy than that expected from electrostatics. Indeed, if the interaction was dominated by

electrostatics, the CO<sub>2</sub> binding energy for V-BTT would be the same as Fe-BTT. The large binding energy for V and Ti is directly related to electronic occupation of their d orbitals, as we now discuss. For the bare framework, the metal atom is five-fold-coordinated and has nearly square pyramidal symmetry. In the absence of CO<sub>2</sub> adsorption, the  $\sigma$  bonds involving the lone pairs of the five coordinating ligands split the d orbitals, as shown in Figure 2. In the present case, the five ligands are the four axial tetrazole nitrogens and the apical chlorine, as described in ref 16.



**Figure 2.** (a) Change of the crystal field splitting upon CO<sub>2</sub> binding from square pyramidal to octahedral for V ( $d^3$ ); dashed lines connecting the change in energy of  $d_z^2$  and the CO<sub>2</sub> lone pair upon adsorption are shown for clarity. (b) Isosurface plot, corresponding to  $0.025 \text{ \AA}^{-3/2}$ , of the wave function (at the  $\Gamma$ -point of the Brillouin zone) corresponding to the metal–CO<sub>2</sub> antibonding orbital. Blue and purple isosurfaces represent positive and negative values, respectively. Gray, blue, red, white, and green atoms are C, N, O, H, and V, respectively.

When CO<sub>2</sub> binds, a coordination-type bond is formed between the metal  $d_z^2$  orbital and one of the oxygen lone pairs of CO<sub>2</sub>, leading to approximately octahedral symmetry about the metal cation. This forces the oxygen lone pair down in energy and the  $d_z^2$  orbital up in energy and results in the formation of a  $\sigma^*$  antibonding state with the CO<sub>2</sub> lone pair. When the electronic occupation of the metal is  $d^2$  and  $d^3$  (for Ti and V), there is a net stabilization upon binding associated with the lowering of the oxygen lone pair energy; because the  $d_z^2$  antibonding molecular orbital is empty, there is no energy penalty when the  $d_z^2$  orbital increases in energy upon adsorption. However, when the metal has an occupation of four or more electrons and is high spin, the scenario changes: an additional d electron is pushed up by roughly the interaction energy between the metal  $d_z^2$  and the oxygen lone pair, reducing the binding energy. For V and Fe, for example, this has a significant consequence: while trends in electrostatic interactions suggest that the CO<sub>2</sub> binding energy would be nearly the same for V and Fe (see Figure 1), the occupied  $d_z^2$  orbital in the Fe case leads to a computed binding energy in Fe-BTT of 47.2 kJ/mol, roughly half the amount calculated for V-BTT (80.2 kJ/mol). The antibonding orbital associated with CO<sub>2</sub> and the metal cation  $d_z^2$  state is shown in Figure 2. This state is occupied for Cr and transition-metal atoms to its right and unoccupied for Ti and V.

When the d electron count is 9 or 10, as for Cu or Zn cations, the  $d_z^2$  orbital becomes doubly occupied and another decrease in binding energy is expected. This is observed, but because of the already weak bond between CO<sub>2</sub> and the metal for  $d \geq 4$ , the double occupation of the antibonding  $\sigma^*$  state

has just a modest effect on the binding energy, comparable to the electrostatic contribution. This leads to a predicted CO<sub>2</sub> binding energy for Cu-BTT of 32.2 kJ/mol, the smallest of all cations considered here, consistent with a doubly occupied  $d_z^2$  orbital and smallest  $Q/r$ . We note that the CO<sub>2</sub> binding energy for Zn-BTT (43.2 kJ/mol) is larger than that for Cr-BTT (36.6 kJ/mol), Co-BTT (39.0 kJ/mol), and Ni-BTT (38.9 kJ/mol) due to the larger electrostatic interaction between CO<sub>2</sub> and Zn. (See Figure 1.)

The lower CO<sub>2</sub> binding strength of Mg and Ca (relative to Ti and V) can be understood by the fact that their 3s and 4s electrons screen the nucleus more effectively than the partially filled 3d electrons of Ti and V ( $d_{xy}$ ,  $d_{xz}$ , and  $d_{yz}$ ), reducing the effective positive charge of alkaline earth cations. (This effect has been recently pointed out by Yu et al. in the context of their calculations of CO<sub>2</sub> binding to MOF-74 MOFs with different metal cations.<sup>25</sup>)

According to the energy diagram shown in Figure 2, we expect that upon CO<sub>2</sub> binding the  $d_z^2$  orbital will shift upward in energy. This is indeed what we observe, as the  $U$ -corrected density of states of V-BTT shows in Figure S2 in the SI. We note that the inclusion of a Hubbard  $U$  does not significantly affect the binding mechanism because the occupation of antibonding  $\sigma^*$  orbitals does not depend on  $U$ .

The bonding mechanism discussed here can be generally applicable to other MOFs with unsaturated open-metal sites possessing similar symmetry. For example, a similar analysis of the CO<sub>2</sub> binding energy in MOF-74 results in essentially the same trend across the first-row transition metals (see SI for detailed results), in agreement with recent works.<sup>13,14</sup> Early first-row transition metals (Ti and V) with empty  $d_z^2$  orbitals show strong binding to CO<sub>2</sub> (53.1 and 62.8 kJ/mol for Ti-MOF-74 and V-MOF-74, respectively). Cr- and Cu-MOF-74 lead to the lowest computed CO<sub>2</sub> binding energies (30.1 and 29.4 kJ/mol, respectively), consistent with occupied  $d_z^2$  orbitals and weak electrostatic contributions. Binding energies at frozen geometries (see SI) show a maximum deviation of 8.5 kJ/mol for V-MOF-74 when a Hubbard  $U$  is included. However, the same trend as a function of the occupation of the d orbitals is found for the  $U$ -corrected binding energies. The robustness of the chemical bonding mechanism proposed here is confirmed by a recent study where a related analysis is used to rationalize large binding energies computed for N<sub>2</sub> and CH<sub>4</sub> to V-MOF74.<sup>26</sup>

In conclusion, we have shown that although the trends in CO<sub>2</sub> binding with open-metal coordination sites are primarily dominated by electrostatic interactions in BTT-type MOFs, binding energies are also highly sensitive to the electronic configuration of the divalent cations. Depending on the metal cation choice, we find that the CO<sub>2</sub> binding energy in BTT can be tuned from a minimum of 32.2 kJ/mol for Cu-BTT to a maximum of 67.2 kJ/mol for Mg-BTT. For Ti and V, however, the CO<sub>2</sub> binding energies are significantly larger than expected from electrostatics arguments (73.2 kJ/mol for Ti-BTT and 80.2 kJ/mol for V-BTT) due to unpopulated antibonding  $\sigma^*$  orbitals formed between the metal  $d_z^2$  orbital and the CO<sub>2</sub> lone pair. For example, replacing Cu with V can increase the CO<sub>2</sub> binding affinity by almost a factor of three. The observation of enhanced CO<sub>2</sub> binding to frameworks with open V and Ti sites also applies to M-MOF-74 and in general any MOF in which the crystal field created upon CO<sub>2</sub> adsorption gives rise to antibonding molecular orbitals that are not populated for a d electron count of 2 or 3, provided that no structural distortions



take place as a function of electron count.<sup>14</sup> More generally, a strong CO<sub>2</sub> affinity with an open-metal site is expected when the  $\sigma^*$  antibonding orbitals between the CO<sub>2</sub> lone pair and metal d orbitals are empty. For example, a crystal field change from square planar to square pyramidal, upon binding, where CO<sub>2</sub> binds apically, can potentially give a larger binding energy for  $d \leq 3$ . Similarly, if a metal geometry changes from tetrahedral to trigonal bipyramidal, upon CO<sub>2</sub> adsorption, a larger binding for  $d \leq 4$  could be obtained. If the metal has a low spin configuration, a larger binding is instead expected for  $d \leq 6$  and  $d \leq 8$ , respectively. This work shows that upon CO<sub>2</sub> binding, that is, upon formation of a  $\sigma$  bond between the CO<sub>2</sub> oxygen and the metal, a chemical bond picture that uses the crystal-field theory and electrostatic considerations of the metal atom, together with the geometry around the metal site, can be used to predict and understand meaningful trends in the CO<sub>2</sub>-MOF binding energy with different open-metal coordination sites. This intuition offers a unique approach to design open-metal site MOFs where, for example, a spin crossover transition could lead to significantly reduced CO<sub>2</sub> desorption energy.

## ■ ASSOCIATED CONTENT

### ■ Supporting Information

Computational details, Mulliken population analysis, density of states, CO<sub>2</sub> binding energies for M-MOF-74; and Hubbard *U* calculations. This material is available free of charge via the Internet at <http://pubs.acs.org>.

## ■ AUTHOR INFORMATION

### Corresponding Authors

\*R.P.: E-mail: roberta.poloni@simap.grenoble-inp.fr.

\*J.B.N.: E-mail: jbnaton@lbl.gov.

### Present Address

#R.F.B.: Department of Chemistry, Western Washington.

### Notes

The authors declare no competing financial interest.

## ■ ACKNOWLEDGMENTS

We thank E. Bloch, K. Sumida, and W. Queen for helpful discussions on BTT MOFs. B.S. was supported by the Center for Gas Separations Relevant to Clean Energy Technologies, an Energy Frontier Research Center funded by the U.S. Department of Energy, Office of Science, Office of Basic Energy Sciences under Award Number DE-SC0001015. K.L. was supported by the U.S. Department of Energy, Office of Basic Energy Sciences, Division of Chemical Sciences, Geosciences and Biosciences under Award DE-FG02-12ER16362. Work at the Molecular Foundry was supported by the Office of Science, Office of Basic Energy Sciences, of the U.S. Department of Energy under Contract No. DE-AC02-05CH11231, and computational resources were provided by DOE (LBNL Lawrence). Work at SIMAP was performed using computing resources from GENCI (CINES and TGCC) (Grant 2013-x2014097211).

## ■ REFERENCES

- (1) IPCC. *IPCC Special Report on Carbon Dioxide Capture and Storage*; Cambridge University Press: Cambridge, U.K., 2005.
- (2) Pacala, S.; Socolow, R. Stabilization Wedges: Solving the Climate Problem for the Next 50 Years with Current Technologies. *Science* **2004**, *305*, 968–972.

- (3) Millward, A. R.; Yaghi, O. M. Metal–Organic Frameworks with Exceptionally High Capacity for Storage of Carbon Dioxide at Room Temperature. *J. Am. Chem. Soc.* **2005**, *127*, 17998–17999.
- (4) Ferèy, G. Hybrid Porous Solids: Past, Present, Future. *Chem. Soc. Rev.* **2008**, *37*, 191–214.
- (5) Morris, R. E.; Wheatley, P. S. Gas Storage in Nanoporous Materials. *Angew. Chem., Int. Ed.* **2008**, *47*, 4966–4981.
- (6) D'Alessandro, D. M.; Smit, B.; Long, J. R. Carbon Dioxide Capture: Prospects for New Materials. *Angew. Chem., Int. Ed.* **2010**, *49*, 6058–6082.
- (7) James, S. L. Metal–Organic Frameworks. *Chem. Soc. Rev.* **2003**, *32*, 276–288.
- (8) Britt, D.; Furukawa, H.; Wang, B.; Glover, T. G.; Yaghi, O. M. Highly Efficient Separation of Carbon Dioxide by a Metal–Organic Framework Replete with Open Metal Sites. *Proc. Natl. Acad. Sci. U.S.A.* **2009**, *106*, 20637–20640.
- (9) Caskey, S. R.; Wong-Foy, A. G.; Metzger, A. J. Dramatic Tuning of Carbon Dioxide Uptake via Metal Substitution in a Coordination Polymer with Cylindrical Pores. *J. Am. Chem. Soc.* **2008**, *130*, 10870–10871.
- (10) Dietzel, P. D. C.; Johnsen, R. E.; Fjellvåg, H.; Bordiga, S.; Groppo, E.; Chavan, S.; Blom, R. Adsorption Properties and Structure of CO<sub>2</sub> Adsorbed on Open Coordination Sites of Metal–Organic Framework Ni<sub>2</sub>(dhtp) from Gas Adsorption, IR spectroscopy and X-ray diffraction. *Chem. Commun.* **2008**, 5125–5127.
- (11) Bloch, E. D.; Britt, D.; Lee, C.; Doonan, C. J.; Uribe-Romo, F. J.; Furukawa, H.; Long, J. R.; Yaghi, O. M. Metal Insertion in a Microporous Metal–Organic Framework Lined with 2,2'-Bipyridine. *J. Am. Chem. Soc.* **2010**, *132*, 14382–14384.
- (12) Valenzano, L.; Civellari, B.; Sillar, K.; Sauer, J. Heats of Adsorption of CO and CO<sub>2</sub> in Metal–Organic Frameworks: Quantum Mechanical Study of CPO-27-M (M = Mg, Ni, Zn). *J. Phys. Chem. C* **2011**, *115*, 21777–21784.
- (13) Park, J.; Kim, H.; Han, S. S.; Jung, Y. Tuning Metal–Organic Frameworks with Open-Metal Sites and its Origin for Enhancing CO<sub>2</sub> Affinity by Metal Substitution. *J. Phys. Chem. Lett.* **2012**, *3*, 826–829.
- (14) Koh, H. S.; Rana, M. K.; Hwang, J.; Siegel, D. J. Thermodynamic Screening of metal-substituted MOFs for Carbon Capture. *Phys. Chem. Chem. Phys.* **2013**, *15*, 4573–4581.
- (15) Grimme, S. Semiempirical GGA-Type Density Functional Constructed with a Long-Range Dispersion Correction. *J. Comput. Chem.* **2006**, *27*, 1787–1799.
- (16) Dincă, M.; Dailly, A.; Liu, Y.; Brown, C. M.; Neumann, D. A.; Long, J. R. Hydrogen Storage in a Microporous Metal–Organic Framework with Exposed Mn<sup>2+</sup> Coordination Sites. *J. Am. Chem. Soc.* **2006**, *128*, 16876–16883.
- (17) Dincă, M.; Han, W. S.; Liu, Y.; Dailly, A.; Brown, C. M.; Long, J. R. Observation of Cu<sup>2+</sup>-H<sub>2</sub> Interactions in a Fully Desolvated Sodalite-Type Metal–Organic Framework. *Angew. Chem., Int. Ed.* **2007**, *46*, 1419–1422.
- (18) Demessence, A.; D'Alessandro, D.; Foo, M. L.; Long, J. R. Strong CO<sub>2</sub> Binding in a Water-Stable, Triazole-Bridged Metal–Organic Framework Functionalized with Ethylenediamine. *J. Am. Chem. Soc.* **2009**, *131*, 8784–8786.
- (19) Sumida, K.; Horike, S.; Kaye, S. S.; Herm, Z. R.; Queen, W. L.; Brown, C. M.; Grandjean, F.; Long, G. J.; Dailly, A.; Long, J. R. Hydrogen Storage and Carbon Dioxide Capture in an Iron-Based Sodalite-Type Metal–Organic Framework (Fe-BTT) Discovered via High-Throughput Methods. *Chem. Sci.* **2010**, *1*, 184–191.
- (20) Poloni, R.; Smit, B.; Neaton, J. B. Ligand-Assisted Enhancement of CO<sub>2</sub> Capture in Metal–Organic Frameworks. *J. Am. Chem. Soc.* **2012**, *134*, 6714–6719.
- (21) Perdew, J. P.; Burke, K.; Ernzerhof, M. Generalized Gradient Approximation Made Simple. *Phys. Rev. Lett.* **1996**, *77*, 3865–3868.
- (22) Soler, J. M.; Artacho, E.; Gale, J. D.; García, A.; Junquera, J.; Ordejón, P.; Sanchez-Portal, D. S. The SIESTA Method for Ab Initio Order-N Materials Simulation. *J. Phys.: Condens. Matter* **2002**, *14*, 2745–2779.

- (23) Poloni, R.; Smit, B.; Neaton, J. B. CO<sub>2</sub> Capture by Metal–Organic Frameworks with van der Waals Density Functionals. *J. Phys. Chem. A* **2012**, *116*, 4957–4964.
- (24) Dincă, M.; Han, W. S.; Liu, Y.; Dailly, A.; Brown, C. M.; Long, J. R. Observation of Cu<sup>2+</sup>–H<sub>2</sub> Interactions in a Fully Desolvated Sodalite-Type Metal–Organic Framework. *Angew. Chem., Int. Ed.* **2007**, *46*, 1419–1422.
- (25) Yu, D.; Yazaydin, A. O.; Lane, J. R.; Dietzel, P. D. C.; Snurr, R. Q. A combined Experimental and Quantum Chemical study of CO<sub>2</sub> Adsorption in the Metal–Organic Framework CPO-27 with Different Metals. *Chem. Sci.* **2013**, *4*, 3544–3556.
- (26) Lee, K.; Isley, W. C.; Dzubak, A. L.; Verma, P.; Stoneburner, S. J.; Howe, J. D.; Bloch, D. E.; Reed, D. A.; Hudson, M. R.; Lin, L.-C.; et al. Design of a Metal–Organic Framework with Enhanced Back Bonding for Separation of N<sub>2</sub> and CH<sub>4</sub>. *J. Am. Chem. Soc.* **2014**, *136*, 698–704.